Materials Research. 2017; 20(4): 984-993
DOI: http://dx.doi.org/10.1590/1980-5373-MR-2016-0618

Effect of Chitosan on the Properties of Electrospun Fibers From Mixed Poly(Vinyl Alcohol)/ Chitosan Solutions

Raquel P. Gonçalves[a], Willian H. Ferreira[a], Rodrigo F. Gouvêa[b], Cristina T. Andrade*[a,b]

[a] Instituto de Macromoléculas Professora Eloisa Mano, Universidade Federal do Rio de Janeiro, Avenida Horácio Macedo 2030, 21941-598 Rio de Janeiro, RJ, Brazil;
[b] Programa de Pós-Graduação em Ciência de Alimentos, Instituto de Química, Universidade Federal do Rio de Janeiro, Avenida Athos da Silveira Ramos 149, 21941-909 Rio de Janeiro, RJ, Brazil.

Received: August 27, 2016; Revised: March 15, 2017; Accepted: May 01, 2017

Electrospun nanofibers were prepared from mixed solutions of partially hydrolyzed poly(vinyl alcohol) (PVA) and medium molar mass chitosan (CS) at different solution compositions, at 15 and 20 kV. The mats were visualized by scanning electron microscopy (SEM), and the average diameters of nanofibers were determined. Three of these solutions were chosen for further studies, to elucidate the influence of CS on the mats properties. Electrospinning at 15 kV had a higher tendency to produce nanofibers free of defects, in which the diameters (157 to 189 nm) were not affected significantly by the total concentration and solution composition. Polymer interactions between the components were supported by infrared spectroscopy, thermogravimetry and dynamic mechanical analysis (DMA). The effect of CS composition was evidenced by DMA and tensile tests techniques. Immersion in water led to the breakage of nanofibers and flower-like morphologies.

Keywords: *Electrospinning, Nanofibers, Chitosan, Poly(vinyl alcohol), Dynamic mechanical analysis*

1. Introduction

Chitosan, the biopolymer produced from chitin deacetylation, has attracted considerable interest for decades. Structurally, chitosan is composed of β-(1,4)-2-amino-2-deoxy-D-glucose and β-(1,4)-2-acetamido-2-deoxy-D-glucose repeating units. Its degree of acetylation and, consequently, the content of amino groups, may be modulated chemically.[1-3] Chitosan is known by its biodegradability and biocompatibility. Also, intrinsic properties of chitosan, such as the antioxidant, antihyperlipidemic, and antibacterial activities were recognized.[4-7] Mainly because of all these properties, chitosan has found numerous applications, especially in the biomedical field, as a polymeric component in drug-release systems and of scaffolds for bone tissue regeneration.[8-10] For healing of skin injuries, the use of nanofibers mats as functional aids is highly recommended. Their high porosity and large surface area mimic the extracellular matrix structure and favor the release of bioactives.[11] In this context, the preparation of chitosan-based mats by electrospinning has received attention.[12]

Electrospinning consists of creating an electrically charged jet, from a drop of a polymer solution or melt, and collecting the resulting material as a loosely connected web of thin fibers. Electrospinning is influenced by many parameters, related to the polymer and solution properties (molar mass, viscosity, surface tension, electrical conductivity), processing conditions (applied electric voltage, tip-to-collector distance, feed rate) and ambient conditions (temperature, humidity).[13-16] In general, to achieve a continuous jet, which would lead to defect-free fibers, high polymer concentrations (around the critical overlap concentration, c*) are necessary.[17] At such concentrations, acid solutions of medium molar mass chitosan show too high viscosities. Electrospinning of these high-viscosity solutions would require the application of high voltages. Also, repulsive forces between ionic groups on the chitosan chains prevent the formation of chain entanglements, necessary for maintaining fiber continuity during jet stretching, whipping and bending, resulting in nanobeads instead of nanofibers.[18] To overcome some of these difficulties, high strength acids, which form stable salts with polycationic chitosan, were used as solvents to electrospin chitosan alone. Under these conditions, the surface tension was reduced and the solution conductivity was increased, which favored the process.[19] Trifluoroacetic acid (TFA), TFA/dichlorometane and formic acid, and concentrated acetic acid (70 – 90%) were used by some authors for chitosan electrospinning.[20-22] However, because of the toxic and corrosive nature of these acids, especially TFA, alternative methods were preferred.[12] Among these methods, the use of mixtures of chitosan and other polymers, such as poly(ethylene oxide) (PEO),[19,23,24] and poly(vinyl alcohol) (PVA) was reported.[25-28]

PVA, a nontoxic, biodegradable and biocompatible polymer, obtained by hydrolysis of poly(vinyl acetate) (PVAc), has found widespread applications in the biomedical field. The electrospinning process of PVA alone from water solution was investigated. The effect of applied electric voltage,

* e-mail: ctandrade@ima.ufrj.br

polymer concentration and of addition of sodium chloride on average fiber diameters and morphology was reported.[29]

In the previously reported data on PVA/CS nanofibers, PVA samples with a high degree of hydrolysis were usually preferred as the component of mixed solutions for electrospinning.[26,28] Also, the characterization of PVA/CS blended nanofibers was not fully explored.[25-28] None of the characterization methods previously reported in the literature led to a straightforward response on the effect of CS on nanofibers properties. To the best of our knowledge, the dynamic mechanical properties of electrospun PVA/CS mats were not investigated. More important, for regenerative applications, such as wound dressing and tissue regeneration, mats are frequently submitted to different types of stress.

In this work, PVA and CS mixed solutions at varied compositions were electrospun under constant processing conditions, at 15 kV and 20 kV. The resulting membranes were visualized by electron scanning microscopy, and carefully evaluated. Homogeneity and fiber average diameters were used to select three of them. The rheological properties of their corresponding solutions were investigated. The selected electrospun mats were submitted to further characterization.

2. Experimental

2.1. Materials

Poly(vinyl alcohol) (PVA) was supplied by Vetec Química Fina (Rio de Janeiro, RJ, Brazil). According to the supplier, this PVA sample has 88% degree of hydrolysis and viscosity-average molecular weight of 85,300. Medium molar mass chitosan (CS) was provided by Sigma Aldrich (São Paulo, SP, Brazil). The degree of acetylation (DA = 15%) of the CS sample was determined by ^{1}H NMR spectrometry in D_2O/DCl at 65ºC. The viscosity-average molecular weight of the CS sample (296,772) was obtained by using the Mark-Houwink equation. The intrinsic viscosity, [η] = 222.95 mL/g, was determined in HAc/NaAc buffer at 25ºC. The constants K = 1.81 x 10^{-3} mL/g and a = 0.93 were used.[30] Analytical grade acetic acid was purchased from Vetec Química Fina Ltda. (Rio de Janeiro, RJ, Brazil).

2.2. Preparation of solutions

Stock-solutions of PVA at 100 g/L in ultrapure water (Milli-Q) and of CS at 25 g/L in 2% (v/v) acetic acid were prepared at room temperature, under stirring for 16 h. Appropriate amounts of the two solutions, at PVA/CS volume ratios of 50:50 (mixture M1), 60:40 (Mixture M2), 70:30 (Mixture M3), 75:25 (Mixture M4), 80:20 (Mixture M5), 75:15 (Mixture M6) and 100:0 (Mixture M7) were mixed and homogenized by heating at 60ºC under stirring for 10 min. Electrospinning of the mixed solutions were carried out no more than 12 h after their preparation.

2.3. Electrospinning

A standard equipment KD Scientific Inc. model 100 (Holliston, MA, USA) was used, which consisted of a syringe pump, a high voltage DC power supply, model PS/FC60PO2.0-11 (Glassman High Voltage Inc., High Bridge, NJ, USA), and a stainless steel plate as collector, previously wrapped in aluminum foil. The mixed solutions were loaded into 5 mL syringes, and pumped through needles of 0.5 mm internal diameter (Hamilton Laboratory Products Inc., Reno, NV, USA) at a rate of 0.5 mL/h, for 15 min. To obtain thick membranes, which could be detached from the aluminum foil and characterized, the experiments were extended for 6 h. Ambient conditions were maintained at 25ºC and 60% relative humidity, and the collector was placed at a distance of 12 cm from the needle tip. The effect of positive output voltages of 15 and 20 kV, applied from the high voltage SC supply, were investigated.

2.4. Characterization of electrospun fibers

Scanning electron microscopy was used to characterize the morphology of the electrospun mats. The samples were visualized with a Jeol electron scanning microscope, model JSM-6460LV (Akishima-shi, Japan), at acceleration voltages of 20 or 10 kV. The surfaces were vacuum-coated with gold before measurements. The SEM images were used to measure fibers average diameters with the Size Meter® software (Laboratório de Controle de Processos, Universidade Federal de Santa Catarina, SC, Brazil). At least, 50 nanofibers were randomly selected from each of the SEM images, and the diameter size distribution was determined with the Origin® software.

Rheological measurements were performed for CS and PVA mixed solutions at 25ºC, 12 h after their preparation, using a controlled stress rheometer AR2000 (TA Instruments Inc., New Castle, DE, USA) fitted with a cone–and–plate geometry, with cone of 40 mm diameter, 2º angle and 54 µm truncation. To determine the linear viscoelastic region, a strain sweep test was performed as the evolution of the complex modulus at 6.28 rad s^{-1}. A frequency sweep step (mechanical spectra) was performed from 10^{-1} to 2 x 10^{2} rad s^{-1} at 5% strain, within the viscoelastic region. Steady state flow was carried out from 10^{-1} to 2 x 10^{2} s^{-1}, and from 2 x 10^{2} s^{-1} to 10^{-1} s^{-1} shear rates. The latter results were considered. The frequency sweep and steady flow experiments were carried out in duplicate to verify the reproducibility of the results. The variation was less than 10%.

Infrared spectroscopy (FTIR) analyses were carried out for the selected mats from 4000 cm^{-1} to 600 cm^{-1}, at ambient temperature, using a Perkin Elmer Frontier spectrometer (Waltham, MA, USA), equipped with an attenuated total reflection accessory (ATR), by averaging 60 scans with a resolution of 4 cm^{-1} in transmission mode.

Thermogravimetric analyses (TGA) were carried out in a TGA Q-500 equipment from TA Instruments. Approximately, 10 mg of sample were heated from 25 to 700ºC, at a 10ºC/min rate, under nitrogen atmosphere.

Dynamic mechanical analyses (DMA) were performed in a Q800 DMA from TA Instruments, equipped with an accessory to measure tensile properties of films. Specimens with 13.0 ± 0.2 mm x 6.0 ± 0.02 mm x 0.09 ± 0.006 mm dimensions were used for the experiments. The dynamic experiments were carried out at 1 Hz in the tensile mode, from −100 to 200°C, at a heating rate of 3°C/min, after conditioning the samples at 25ºC and 50% relative humidity, for a period of at least 48 h. During the experiments, the strain amplitude was kept at 0.1% to ensure a linear viscoelastic response from the sample. The data were expressed as the variation of the storage modulus (E') as a function of temperature, and the variation of the loss factor, given by the ratio between the loss modulus (E") and E' as a function of temperature.

Uniaxial tensile tests were performed in the same Q800 equipment, at 25ºC, with a force of 1 N. The average value was taken from a total of three measurements.

Immersion tests were performed with electrospun specimens of 5 cm in length and 1 cm in width. The specimens were treated in 25 mL water for 12 h. Then, the resulting membranes were dried and analyzed by SEM.

2.5. Statistical analysis

Statistical analyses were performed to evaluate the fiber average diameters of PVA/CS electrospun nanofibers. Results were expressed as mean ± standard deviation. One-way analysis of variance (ANOVA) was applied to the data by using Statistica® v.8 software. A p-value equal or less than 0.05 was considered significant. The Fisher's test was used to compare the average diameters of the samples.

3. Results and Discussion

3.1. Morphological characterization

In preliminary experiments, the possibility of dispersing the PVA sample in water and the CS sample in 2% acetic acid at higher concentrations failed. The resulting solutions had very high viscosities, which made manipulation nearly impossible. The highest suitable concentrations of CS and PVA stock solutions, which allowed the preparation of the mixtures, were chosen for the study. Parameters, such as flow rate, working distance and voltage were adjusted in preliminary experiments. To better investigate the electrospinning behavior of the mixtures and the morphology of the resulting mats, PVA and CS mixed solutions were electrospun at 15 and 20 kV. At first, the 15 kV condition was discouraging, because electrospinning of other CS/PVA aqueous solutions had been previously carried out at 15 kV, and the reported SEM images of the blended fibers were not free of defects.[31] Figure 1 shows the SEM images obtained for the M1 – M7 membranes, resulting from the electrospinning of PVA/CS mixed solutions.

In Figure 1a, film formation may be visualized above and below the web of fibers and bead defects. Beads are frequently observed when polymer chains do not form a conveniently deformable entangled network for conventional electrospinning. The origin of film formation may be attributed to the evaporation of residual solvent not vaporized during the process, and that remained encapsulated within fibers.[24] Apparently, the increase in the applied voltage from 15 kV to 20 kV reduced film formation in M1 (Figure 1a1), but did not prevent the formation of regular and irregular beads (Figure 1a1). Because of film formation and bead imperfections, the M1 mats were not considered for further studies. Figure 2 and Table 1 show that the average fiber diameters varied from 129 nm to 189 nm, and from 127 nm to 181 nm, for PVA/CS mats electrospun at 15 kV and 20 kV, respectively.

According to some reported data, at least for poly(lactic acid), solutions at lower polymer concentrations give rise to electrospun fibers with smaller diameters.[32] This behavior was observed for the M2 mat, prepared from the lowest total concentration, and that presented the lowest average diameter. However, the M2 behavior was exception in relation to the other mats. It is worth observing that, in the case of PVA/CS mats of this work, as the content of PVA increased, the total polymer concentration also increased. At 20 kV, the total polymer concentration and CS composition affected significantly the fiber diameter (Figure 2 and Table 1). Surprisingly, no such effect was observed at 15 kV for M3, M4, M5 and M6 mats from PVA/CS mixed solutions. This result indicated that, at 15 kV, the total mixture concentration and composition did not affect the average nanofiber diameter. Also, it is worth observing in Figure 1(b-f) that defect-free fibers tend to be formed preferentially at 15 kV (Figure 1b-f). Because of the unexpected result on the statistically equal diameters of their nanofibers, three mixed solutions (M3, M4 and M6) were chosen to be characterized by rheological tests. Also, these mixtures were electrospun for longer periods of time at 15 kV and the resulting mats were further characterized.

3.2. Rheological characterization of mixed solutions for electrospinning

PVA/CS mixed solutions were optically clear, transparent and homogeneous, which denoted miscibility between the two polymers. The viscoelasticity of the M3, M4 and M6 solutions was studied by dynamic measurements at 25ºC. The mechanical spectra (Figure 3a) revealed their liquid-like character; the loss modulus (G") values were higher than the storage modulus (G') values along the range of oscillatory frequencies investigated. The M3 sample, which resulted from the mixture of PVA and

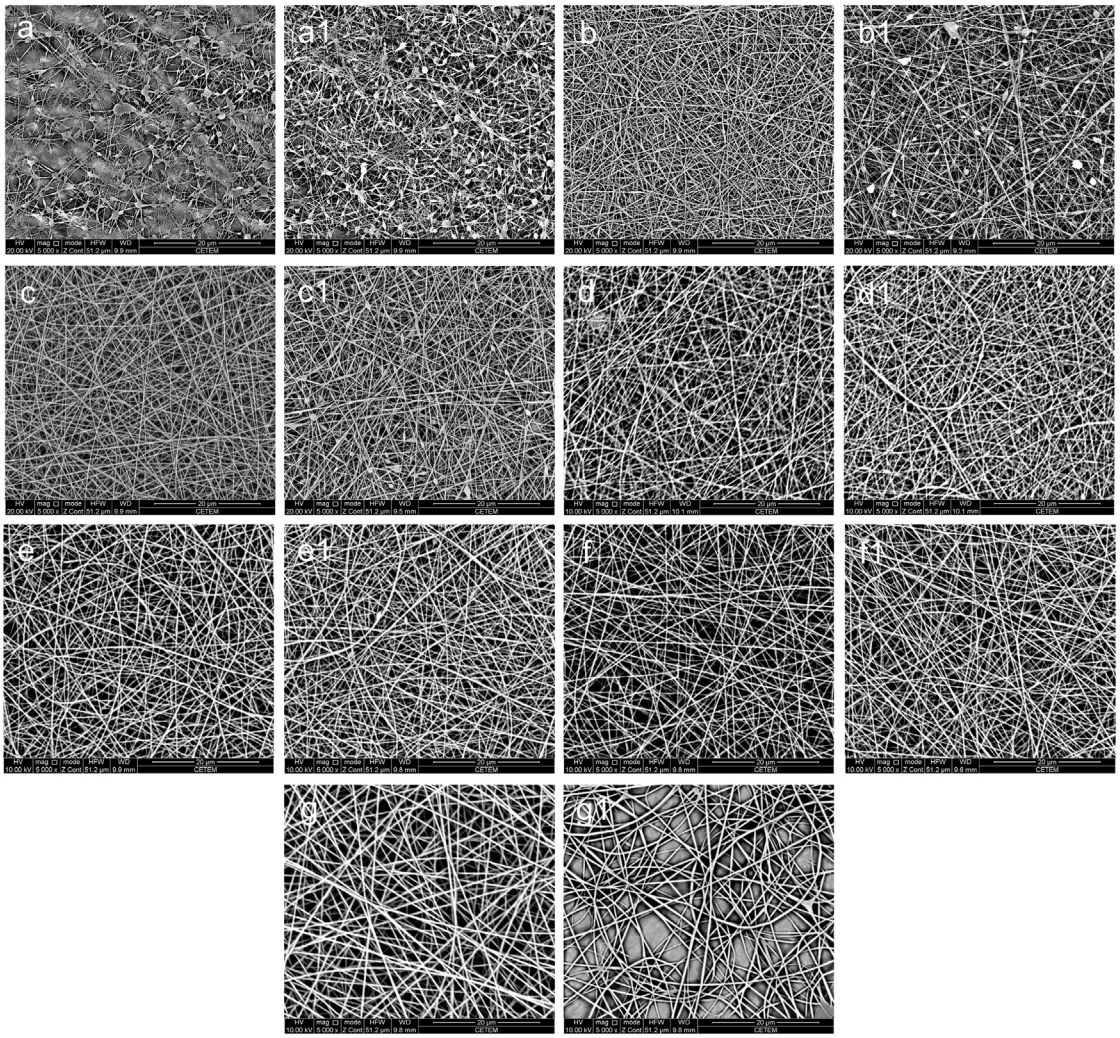

Figure 1. SEM images for PVA/CS nanofibers electrospun at 15 and 20 kV, respectively, from mixed solutions at 50:50 (mixture M1; a, a1), 60:40 (mixture M2; b, b1), 70:30 (mixture M3; c, c1), 75:25 (mixture M4; d, d1), 80:20 (mixture e, e1), 85:15 (mixture M6; f, f1), 100:0 (mixture M7; g, g1) compositions.

CS stock solutions at a 70:30 volume ratio, showed the typical behavior of a dilute system, without a G' - G" crossover. No crossover was observed for the other two samples also. However, the crossover for M4 and M6 may be envisaged around 3 x 10^3 rads/s and 9 x 10^2 rad/s, respectively. This decrease in the crossover frequency was expected, and reflected the increase in total concentration, as the PVA composition was increased in the mixed solutions. The variation of viscosity as a function of shear rate was investigated for the samples (Figure 3b). A shear-thinning, pseudoplastic behavior was observed, which usually characterizes polymer solutions and dispersions. As expected, the viscosity values increased as the total composition increased.

3.3. Infrared spectroscopy (FTIR)

FTIR spectra were obtained for CS and PVA as powders (Figure 4a, traces I and II, respectively), and for the M3, M4 and M6 mats (Figure 4b, traces I, II and III, respectively). For the CS sample, the broad absorption in the range ~ 3600 cm^{-1} to 3000 cm^{-1} was assigned to O−H and N−H stretching vibrations. The absorptions at 1658 cm^{-1} and 1590 cm^{-1} were attributed, respectively, to the amide I (C=O stretching) and amide II (C–N stretching and C–N–H bending vibrations) of amide functional groups in the solid state. For PVA, the absorption corresponding to the O−H stretching was observed at 3304 cm^{-1}. The band at 1714 cm^{-1} was attributed to C=O stretching of nonhydrolyzed vinyl acetate groups. The absorptions in the range 2930 – 2910 cm^{-1}, present in all spectra, were attributed to C−H stretching vibrations. The C−O asymmetric stretching band, which also appeared in the spectra obtained for all samples, was visualized around 1100 cm^{-1}. Particularly for the mats, in relation to PVA, the O−H stretching was shifted to higher wavenumbers (3310

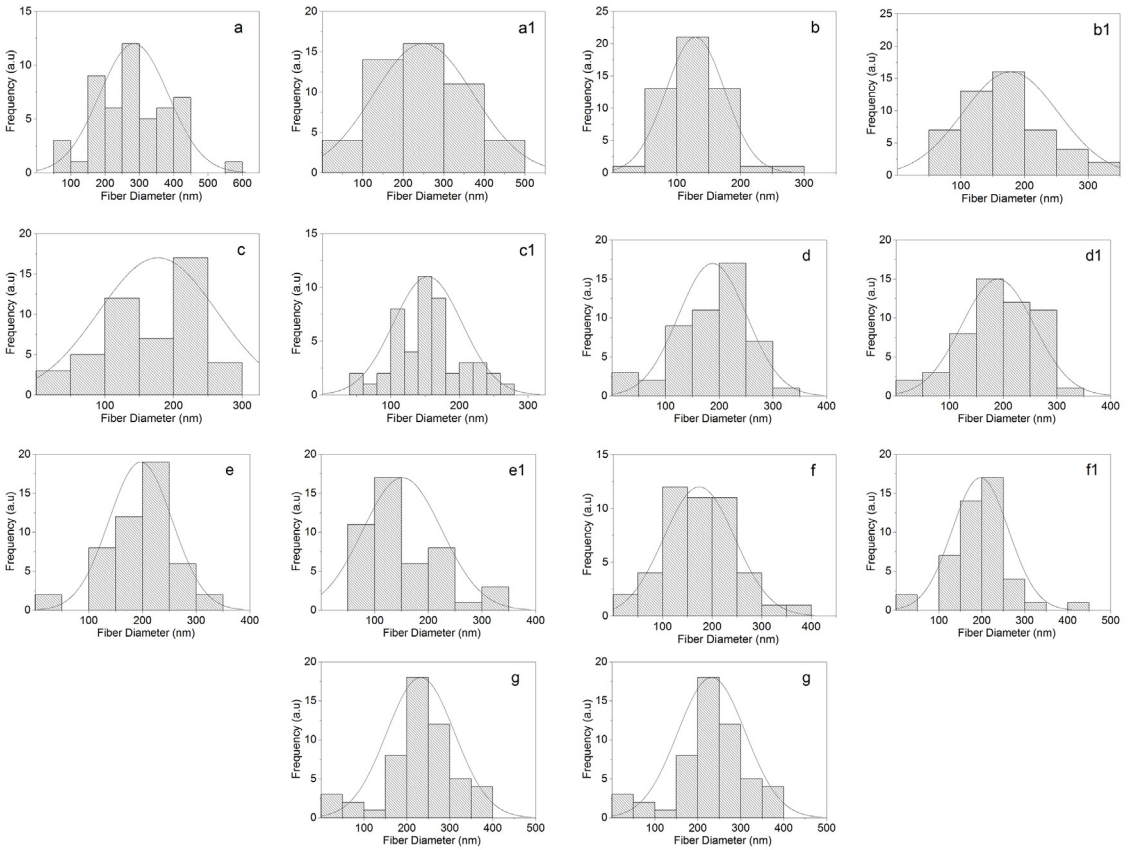

Figure 2. Diameter distributions for PVA/CS nanofibers electrospun at 15 and 20 kV, respectively, from mixed solutions at 50:50 (mixture M1; a, a1), 60:40 (mixture M2; b, b1), 70:30 (mixture M3; c, c1), 75:25 (mixture M4; d, d1), 80:20 (mixture e, e1), 85:15 (mixture M6; f, f1), 100:0 (mixture M7; g, g1) compositions.

Table 1. Fiber average diameters for PVA/CS mats

Sample	PVA:CS volume ratio	Fiber average diameter* at 15 kV (μm)	Fiber average diameter* at 20 kV (μm)
M1	50:50	0.284 ± 0.100^{a}	0.231 ± 0.137^{a}
M2	60:40	0.129 ± 0.046^{b}	$0.178 \pm 0.075^{b,c}$
M3	70:30	0.166 ± 0.095^{c}	0.148 ± 0.058^{b}
M4	75:25	0.188 ± 0.064^{c}	$0.180 \pm 0.079^{c,d}$
M5	80:20	0.189 ± 0.069^{c}	0.127 ± 0.088^{b}
M6	85:15	0.157 ± 0.086^{c}	$0.181 \pm 0.083^{c,d}$
M7	100:0	0.232 ± 0.079^{d}	0.316 ± 0.116^{e}

*Average diameters on the same column and with the same letter do not differ to the 5% level of significance.

– 3330 cm^{-1}), whereas in relation to CS, the shift was to lower wavenumbers. This result might be an indication of the formation of extensive intermolecular hydrogen bonds between PVA and CS chains. Some authors reported the disappearance of the band at 1255 cm^{-1} in CS/PVA mats, as an indication of the formation of hydrogen bonds between the components.[26] However, as can be observed in Figure 4, the band located around 1250 cm^{-1} appeared in the spectra obtained for PVA and for the PVA/CS mats.

3.4. Thermogravimetric analysis (TGA)

TGA was used to investigate the thermal stability of the M3, M4 and M6 samples (Figure 5 a,b). The thermal degradation curves obtained for the mats followed the same profile, in three stages. As usually found for hydrophilic polymers, the first event (50ºC – 100ºC) was attributed to the loss of moisture; in this case, approximately 10 mass%. The second stage, which extended from 250ºC to 390ºC, had maximum degradation rate at T_{max} = 315ºC, as can

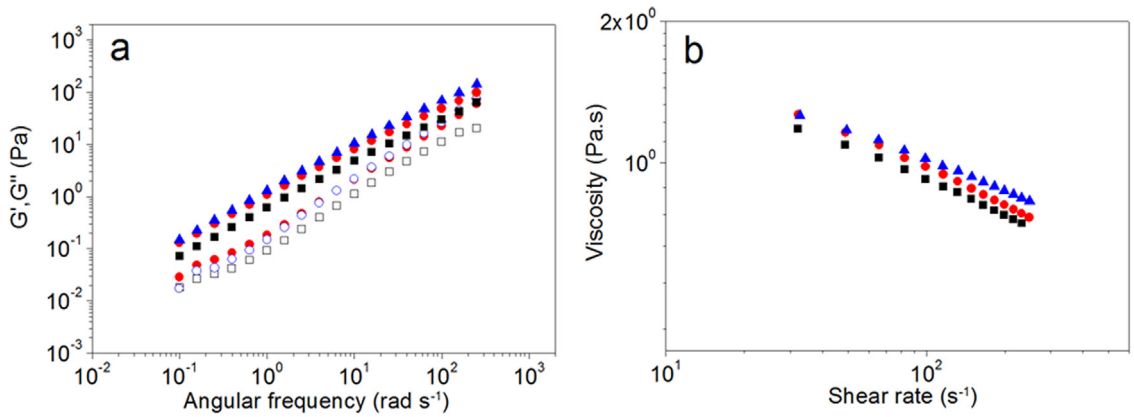

Figure 3. Storage modulus (open symbols) and loss modulus (full symbols) *versus* oscillation frequency at 25ºC and 5% strain amplitude (a), and viscosity versus shear rate at 25ºC and 5% strain amplitude (b), for the PVA/CS mixed solutions at 70:30 (squares), 75:25 (circles) and 85:15 (triangles) compositions, precursors of M3, M4 and M6 mats.

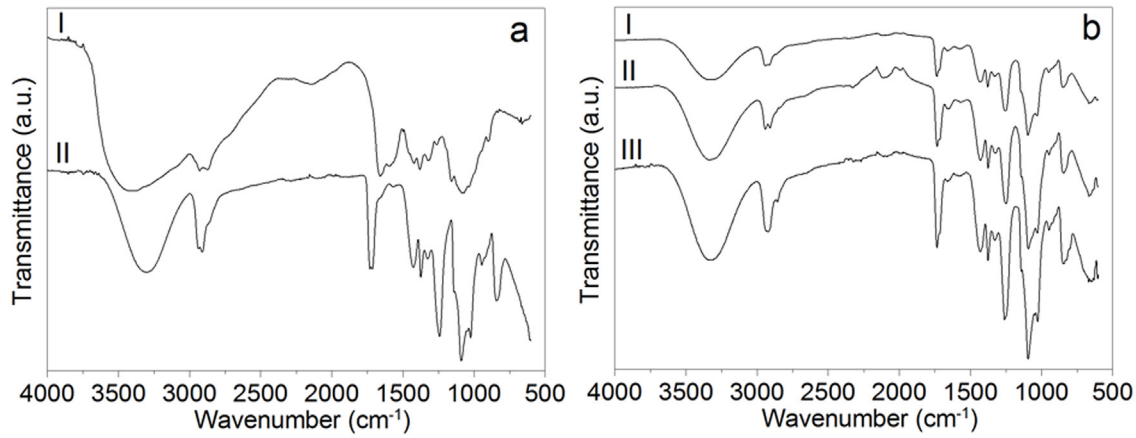

Figure 4. FTIR spectra for (a) chitosan (CS, trace I) and poly(vinyl alcohol) (PVA, trace II); (b) PVA/CS mats at 70:30 (M3, trace I), 75:25 (M4, trace II) and 85:15 (M6, trace III) compositions.

be observed in the DTG curves of Figure 5b. It is worth observing that CS alone (result not shown) showed the main thermal degradation in the range 273ºC to 375ºC, with T_{max} = 293ºC, consistent with a recently reported result for CS,[33] and significantly lower than that observed for the mats. Also, the TG curve for PVA alone showed three stages of mass loss. These stages were attributed to moisture loss, polymer dehydration and formation of polyacetylene-like structures (200ºC – 400ºC).[34] Finally, around 400ºC and 550ºC, the decomposition of PVA main chain would occur, leading to the release of carbon dioxide gas and formation of oxides.[34] However, besides the peak with T_{max} at 430ºC, no resolution of the peak with T_{max} = 315ºC was observed in Figure 5b. The appearance of the shoulder at 360ºC might be another indication of intermolecular interaction, stabilized by hydrogen bonds, between PVA and CS macromolecular chains.

3.5. Dynamic mechanical analysis (DMA)

Dynamic mechanical analyses were carried out for the M3, M4 and M6 mats (Figure 6). Figure 6a shows the variation of the loss factor (tan δ) as a function of temperature. Two relaxations, β and α, were observed in the curves. The first, located around –5.6ºC, had its intensity reduced as the composition of PVA decreased in the samples. This β relaxation is associated to motions of substituent groups, linked to polymers main chains. It is interesting to note that a similar event was also observed at –14.5ºC for a chitosan film (not electrospun) of medium molar mass.[35] The occurrence of the β relaxation for the M3, M4 and M6 mats at a higher temperature might be explained as a result of the decreasing mobility of substituent groups of interacting PVA and CS. Also, the higher intensity of the β relaxation observed for the M6 sample confirmed that, in this mat mainly composed of

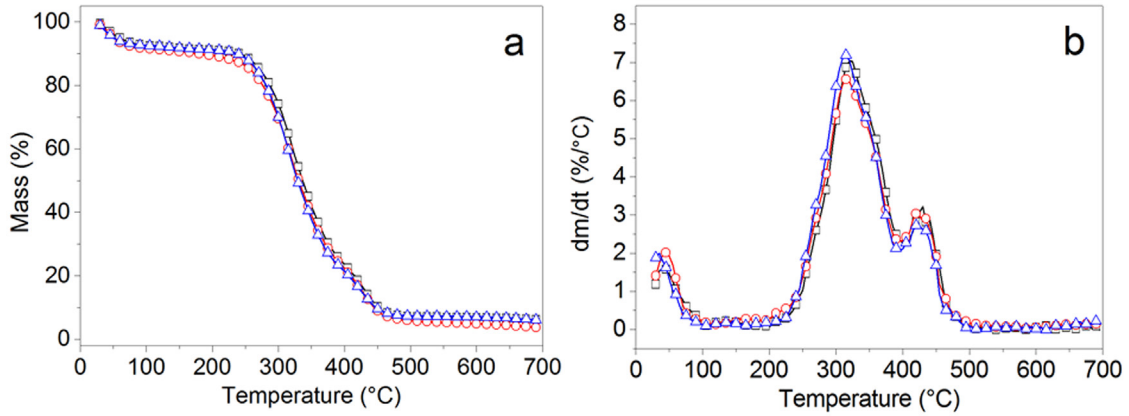

Figure 5. TG (a) and DTG (b) curves for PVA/CS mats at 70:30 (M3, squares), 75:25 (M4, circles), and 85:15 (M6, triangles) compositions.

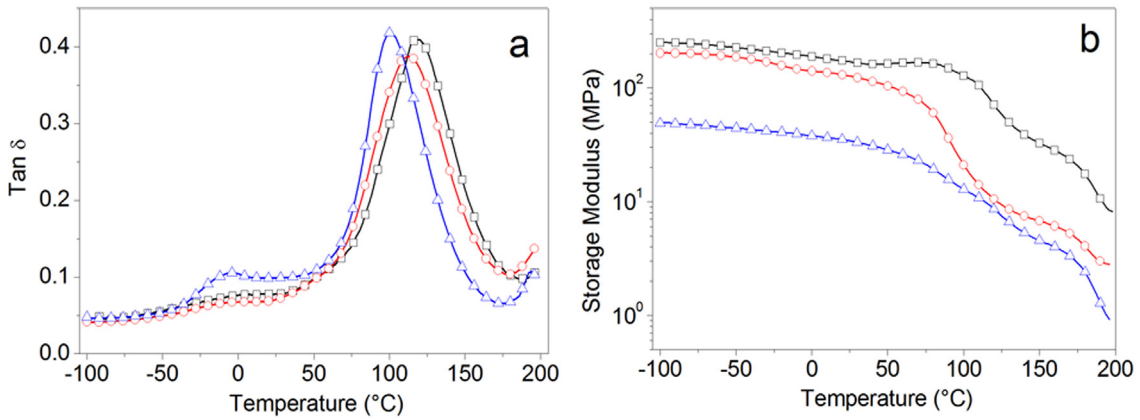

Figure 6. Tangent delta (a) and storage modulus values (b) as a function of temperature for PVA/CS mats at 70:30 (M3, squares), 75:25 (M4, circles) and 85:15 (M6, triangles) compositions.

PVA, the substituent groups are much less constrained than the substituent groups in M3 and M4. The other more intense peak in the tan δ curves is attributed to the α relaxation and is associated to the dynamic glass transition temperature, which is generally higher than the T_g observed by DSC.[36] For the M6 sample, with the highest composition of PVA, this peak was observed at 100ºC. This peak was broader and shifted to higher temperatures, around 110ºC and 125ºC, respectively, for M4 and M3, with higher compositions of CS. Similarly, data reported by other authors on the DMA properties of PVA,[37] and chitosan films alone,[35] revealed expressively lower T_g values (25ºC and 46.8ºC, respectively). This behavior suggested restricted segmental motions in the amorphous region of the mats, and corroborated FTIR and TGA data, on the idea that these nanofibers are formed by interacting PVA and CS macromolecules.

Figure 6b shows the evolution of the storage modulus (E') as a function of temperature for the M3, M4 and M6 samples. At low temperatures, in the glassy state, E' decreased gradually as the temperature was increased. The amount of CS in the mats had an expressive influence on E' behavior. CS contributed to improve the elastic response along the

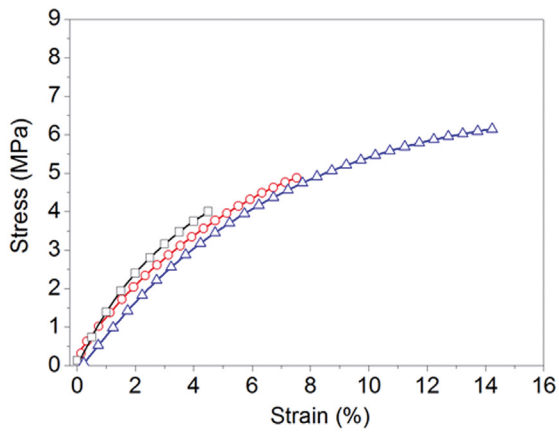

Figure 7. Stress versus strain curves for PVA/CS mats at 70:30 (M3, squares), 75:25 (M4, circles) and 85:15 (M6, triangles) compositions.

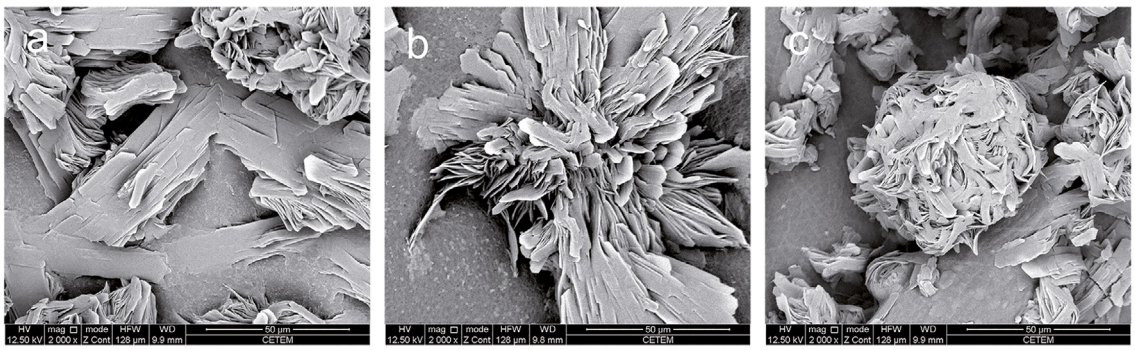

Figure 8. SEM images for PVA/CS mats at 70:30 (M3, a), 75:25 (M4, b) and 85:15 (M6, c) compositions, after immersion in water.

temperature range studied. The E' values recorded at 25ºC were 34 MPa, 128 MPa and 167 MPa for M6, M4 and M3, respectively. The M3 mat, with the highest content of CS, maintained higher E' values even at its T_g, at 125ºC. This stiffening effect indicated the more restricted segmental motions in M3 macromolecules, when compared to the other mats, and confirmed the occurrence of intermolecular PVA/CS interactions, as detected by FTIR and TGA results.

3.6. Tensile tests

The mechanical properties of the M3, M4 and M6 mats were investigated by uniaxial tensile tests, and the stress *versus* strain curves are shown in Figure 7. As expected, the mechanical parameters found for the mats were lower than those reported for a bulk film of medium molar mass CS, analyzed by a similar methodology.[35] The highest Young's modulus (E = 201.7 ± 13.2 MPa), the lowest elongation at break (ε_{max} = 3.96 ± 0.45%) and tensile stress at break (σ_{max} = 4.15 ± 0.41 MPa) were determined for the M3 mat. This result indicated that CS contributed to the hardness and brittleness of this sample. With increasing PVA contents, expressive differences were observed. The M4 sample presented intermediate values of E = 173.6 ± 12.6 MPa, σ_{max} = 4.97 ± 0.53 and ε_{max} = 7.53 ± 0.87%. The highest ductibility was obtained for M6, with the highest composition of PVA, for which E = 94.2 ± 10.2 MPa, σ_{max} = 6.13 ± 0.72 MPa and ε_{max} = 14.13 ± 1.25%. The highest value of ε_{max}, found for the PVA-richest sample, characterized the most flexible mat.

3.7. Immersion of PVA/CS electrospun membranes in water

The M3, M4 and M6 samples were immersed in water to investigate how their composition interfered on their morphology, after a possible dissolution of PVA. Other authors also reported on PVA extraction from mixed PVA/CS nanofibers, resulting in different morphologies. In the first work, the PVA/CS nanofibers, prepared with a high molar mass PVA, were treated with aqueous NaOH. The pores and holes observed by the authors were attributed to phase separation.[25] On the other hand, extraction of a high molar mass PVA (degree of hydrolysis 98 - 99%) with 0.5 M NaOH from PVA/CS mats led to nanofibers with decreasing diameters, from 150 – 300 nm to 80 – 150 nm.[38] Contrarily, in this study, no fibers could be observed. In the SEM images of the water-treated and dried membranes (Figure 8), broken nanofibers were agglomerated and transformed into sheets. This result seems to indicate that, at the breakage points, fibers were formed by PVA macromolecules alone, whereas the remaining sheets, resulting from nanofibers agglomeration, consisted of PVA and CS interacting macromolecules. Probably, the agglomeration of nanofibers was caused by swelling of PVA molecules, followed by adhesion of the PVA/CS fibers. For M3 and M4 (Figure 8a and 8b, respectively), the rigidity detected by DMA and by tensile tests was reflected in the flower-like structures, which are clearly more rigid than those observed for the water-treated M6 sample (Figure 8c). In the latter case, although sheets were also visualized, their flexibility was evidenced by their inward features.

4. Conclusions

Electrospun nanofibers were prepared at 15 and 20 kV from mixed solutions of partially hydrolyzed poly(vinyl alcohol) and medium molar mass chitosan. SEM images showed that nanofibers prepared at 15 kV had a higher tendency to be free of defects. For these fibers, their diameters were not significantly affected by polymer total concentration and solution composition. The rheological properties of selected mixed solutions were dependent only on the total polymer concentration, which varied from 7.75 to 8.50 %. FTIR, TGA and DMA results gave evidence of intermolecular interactions between the functional groups of the polymeric constituents. Important information on the role of chitosan on the mats properties were provided by the results from DMA and tensile tests. This conclusion is relevant because of the low concentrations of chitosan (0.75 to 0.5%) and the small difference between them. Depending on the application, the composition of chitosan could be balanced to achieve the desirable performance. Although excess of poly(vinyl alcohol) contributes to mats formation and flexibility, its high solubility in water limits its use.

5. Acknowledgements

The authors acknowledge Conselho Nacional de Desenvolvimento Científico e Tecnológico (CNPq) (Grant Nº 471676/2013-6) for financial support.

6. References

1. Lamarque G, Viton C, Domard A. Comparative Study of the first Heterogeneous Deacetylation of α- and β-Chitins in a Multistep Process. *Biomacromolecules*. 2004;5(3):992-1001. DOI: 10.1021/bm034498j

2. Lamarque G, Lucas JM, Viton C, Domard A. Physicochemical Behavior of Homogeneous Series of Acetylated Chitosans in Aqueous Solution: Role of Various Structural Parameters. *Biomacromolecules*. 2005;6(1):131-142. DOI: 10.1021/bm0496357

3. Liu L, Zhou S, Wang B, Xu F, Sun R. Homogeneous acetylation of chitosan in ionic liquids. *Journal of Applied Polymer Science*. 2012;129(1):28-35. DOI: 10.1002/app.38701

4. Ngo DH, Vo TS, Ngo DN, Kang KH, Je JY, Pham HND, et al. Biological effects of chitosan and its derivatives. *Food Hydrocolloids*. 2015;51:200-216. DOI: 10.1016/j.foodhyd.2015.05.023

5. Anraku M, Fujii T, Kondo Y, Kojima E, Hata T, Tabuchi N, et al. Antioxidant properties of high molecular weight dietary chitosan in vitro and in vivo. *Carbohydrate Polymers*. 2011;83(2):501-505. DOI: 10.1016/j.carbpol.2010.08.009

6. Katiyar D, Singh B, Lall AM, Haldar C. Efficacy of chitooligosaccharides for the management of diabetes in alloxan induced mice: A correlative study with antihyperlipidemic and antioxidative activity. *European Journal of Pharmaceutical Sciences*. 2011;44:534-543. DOI: 10.1016/j.ejps.2011.09.015

7. Fernandes JC, Tavaria FK, Soares JC, Ramos OS, Monteiro MJ, Pintado ME, et al. Antimicrobial effects of chitosans and chitooligosaccharides, upon *Staphylococcus aureus* and *Escherichia coli*, in food model systems. *Food Microbiology*. 2008;25(7):922-928. DOI: 10.1016/j.fm.2008.05.003

8. Du H, Liu M, Yang X, Zhai G. The design of pH-sensitive chitosan-based formulations for gastrointestinal delivery. *Drug Discovery Today*. 2015;20(8):1004-1011. DOI: 10.1016/j.drudis.2015.03.002

9. Prabaharan M. Chitosan-based nanoparticles for tumor-targeted drug delivery. *International Journal of Biological Macromolecules*. 2015;72:1313-1322. DOI: 10.1016/j.ijbiomac.2014.10.052

10. Basha RY, Kumar S, Doble M. Design of biocomposite materials for bone tissue regeneration. *Materials Science and Engineering: C*. 2015;57:452-463. DOI: 10.1016/j.msec.2015.07.016

11. Matthews JA, Wnek GE, Simpson DG, Bowlin GL. Electrospinning of Collagen Nanofibers. *Biomacromolecules*. 2002;3(2):232-238. DOI: 10.1021/bm015533u

12. Elsabee MZ, Naguib HF, Morsi RE. Chitosan based nanofibers, review. *Materials Science and Engineering: C*. 2012;32(7):1711-1726. DOI: 10.1016/j.msec.2012.05.009

13. Doshi J, Reneker DH. Electrospinning process and applications of electrospun fibers. *Journal of Electrostatics*. 1995;35(2-3):151-160. DOI: 10.1016/0304-3886(95)00041-8

14. Agarwal S, Wendorff JH, Greiner A. Use of electrospinning technique for biomedical applications. *Polymer*. 2008;49(26):5603-5621. DOI: 10.1016/j.polymer.2008.09.014

15. Ghorani B, Tucker N. Fundamentals of electrospinning as a novel delivery vehicle for bioactive compounds in food nanotechnology. *Food Hydrocolloids*. 2015;51:227-240. DOI: 10.1016/j.foodhyd.2015.05.024

16. Salles THC, Lombello CB, d'Ávila MA. Electrospinning of Gelatin/Poly (Vinyl Pyrrolidone) Blends from Water/Acetic Acid Solutions. *Materials Research*. 2015;18(3):509-518. DOI: 10.1590/1516-1439.310114

17. McKee MG, Wilkes GL, Colby RH, Long TE. Correlations of Solution Rheology with Electrospun Fiber Formation of Linear and Branched Polyesters. *Macromolecules*. 2004;37(5):1760-1767. DOI: 10.1021/ma035689h

18. Min BM, Lee SW, Lim JN, You Y, Lee TS, Kang PH, et al. Chitin and chitosan nanofibers: electrospinning of chitin and deacetylation of chitin nanofibers. *Polymer*. 2004;45(21):7137-7142. DOI: 10.1016/j.polymer.2004.08.048

19. Klossner RR, Queen HA, Coughlin AJ, Krause WE. Correlation of Chitosan's Rheological Properties and Its Ability to Electrospin. *Biomacromolecules*. 2008;9(10):2947-2953. DOI: 10.1021/bm800738u

20. Ohkawa K, Cha D, Kim H, Nishida A, Yamamoto H. Electrospinning of Chitosan. *Macromolecular Rapid Communications*. 2004;25(18):1600-1605. DOI: 10.1002/marc.200400253

21. Ohkawa K, Minato KI, Kumagai G, Hayashi S, Yamamoto H. Chitosan Nanofiber. *Biomacromolecules*. 2006;7(11):3291-3294. DOI: 10.1021/bm0604395

22. Homayoni H, Ravandi SAH, Valizadeh M. Electrospinning of chitosan nanofibers: Processing optimization. *Carbohydrate Polymers*. 2009;77(3):656-661. DOI: 10.1016/j.carbpol.2009.02.008

23. Pakravan M, Heuzey MC, Ajji A. A fundamental study of chitosan/PEO electrospinning. *Polymer*. 2011;52(21):4813-4824. DOI: 10.1016/j.polymer.2011.08.034

24. Cheng F, Gao J, Wang L, Hu X. Composite chitosan/poly(ethylene oxide) electrospun nanofibrous mats as novel wound dressing matrixes for the controlled release of drugs. *Journal of Applied Polymer Science*. 2015;132(24). DOI: 10.1002/app.42060

25. Li L, Hsieh YL. Chitosan bicomponent nanofibers and nanoporous fibers. *Carbohydrate Research*. 2006;341(3):374-381. DOI: 10.1016/j.carres.2005.11.028

26. Jia YT, Gong J, Gu XH, Kim HY, Dong J, Shen XY. Fabrication and characterization of poly(vinyl alcohol)/chitosan blend nanofibers produced by electrospinning method. *Carbohydrate Polymers*. 2007;67(3):403-409. DOI: 10.1016/j.carbpol.2006.06.010

27. Hadipour-Goudarzi E, Montazer M, Latifi M, Aghaji AAG. Electrospinning of chitosan/sericin/PVA nanofibers incorporated within situ synthesis of nano silver. *Carbohydrate Polymers*. 2014;113:231-239. DOI: 10.1016/j.carbpol.2014.06.082

28. Farooq A, Yar M, Khan AS, Shahzadi L, Siddiqi SA, Mahmood N, et al. Synthesis of piroxicam loaded novel electrospun biodegradable nanocomposite scaffolds for periodontal regeneration. *Materials Science and Engineering: C*. 2015;56:104-113. DOI: 10.1016/j.msec.2015.06.006

29. Zhang C, Yuan X, Wu L, Han Y, Sheng J. Study on morphology of electrospun poly(vinyl alcohol) mats. *European Polymer Journal*. 2005;41(3):423-432. DOI: 10.1016/j.eurpolymj.2004.10.027

30. Kaya M, Asan-Ozusaglam M, Erdogan S. Comparison of antimicrobial activities of newly obtained low molecular weight scorpion chitosan and medium molecular weight commercial chitosan. *Journal of Bioscience and Bioengineering*. 2016;121(6):678-684. DOI: 10.1016/j.jbiosc.2015.11.005

31. Zhang Y, Huang X, Duan B, Wu L, Li S, Yuan X. Preparation of electrospun chitosan/poly(vinyl alcohol) membranes. *Colloid and Polymer Science*. 2007;285(8):855-863. DOI: 10.1007/s00396-006-1630-4

32. Tan SH, Inai R, Kotaki M, Ramakrishna S. Systematic parameter study for ultra-fine fiber fabrication via electrospinning process. *Polymer*. 2005;46(16):6128-6134. DOI: 10.1016/j.polymer.2005.05.068

33. Zhang H, Luo X, Lin X, Lu X, Zhou Y, Tang Y. Polycaprolactone/chitosan blends: Simulation and experimental design. *Materials & Design*. 2016;90:396-402. DOI: 10.1016/j.matdes.2015.10.108

34. Mallakpour S, Abdolmaleki A, Khalesi Z, Borandeh S. Surface functionalization of GO, preparation and characterization of PVA/TRIS-GO nanocomposites. *Polymer*. 2015;81:140-150. DOI: 10.1016/j.polymer.2015.11.005

35. Bof MJ, Bordagaray VC, Locaso DE, García MA. Chitosan molecular weight effect on starch-composite film properties. *Food Hydrocolloids*. 2015;51:281-294. DOI: 10.1016/j.foodhyd.2015.05.018

36. Lewandowska K. Miscibility and thermal stability of poly(vinyl alcohol)/chitosan mixtures. *Thermochimica Acta*. 2009;493(1-2):42-48. DOI: 10.1016/j.tca.2009.04.003

37. Cho MJ, Park BD. Tensile and thermal properties of nanocellulose-reinforced poly(vinyl alcohol) nanocomposites. *Journal of Industrial and Engineering Chemistry*. 2011;17(1):36-40. DOI: 10.1016/j.jiec.2010.10.006

38. Huang XJ, Ge D, Xu ZK. Preparation and characterization of stable chitosan nanofibrous membrane for lipase immobilization. *European Polymer Journal*. 2007;43(9):3710-3718. DOI: 10.1016/j.eurpolymj.2007.06.010